

DYNAMICS OF THE MOBILE WHEELED PENDULUM

ȘTEFAN STAICU

Abstract. Kinematics and the dynamics analysis of a two-wheeled mobile robot comprising an oscillating intermediate central body are established in the paper. The dynamics of this mechanical system is formulated using the fundamental principle of virtual work, but it has been verified the results in the framework of the Lagrange formalism with their multipliers. The study of the dynamics problems of the wheeled mobile robots is done mainly to solve successfully the control of the motion of such systems

LIST OF SYMBOLS

- $Ox_0y_0z_0$ – inertial reference frame with origin in the ground surface
 $a_{k,k-1}$ – orthogonal transformation matrix
 $\vec{u}_1, \vec{u}_2, \vec{u}_3$ – three right-handed orthogonal unit vectors
 θ_1, θ_2 – rotation angles of two driving wheels
 θ_3 – inclination angle of the intermediate central body
 l – distance between the wheel centres
 $d = C_2G$ – displacement of the mass centre G of the central body
 r – radius of each wheel
 $\vec{r}_{21}^A, \vec{r}_{21}^B$ – relative position vectors of wheel centres
 ψ, x_{10}, y_{10}, r – orientation angle and centre coordinates of a fictitious platform linking the wheels
 $\vec{\omega}_{k,k-1}$ – relative angular velocity of T_k
 $\vec{\omega}_{k0}$: absolute angular velocity of T_k
 $\tilde{\omega}_{k,k-1}$ – skew-symmetric matrix associated to the angular velocity $\vec{\omega}_{k,k-1}$
 $\vec{\mathcal{E}}_{k,k-1}$ – relative angular acceleration of T_k
 $\vec{\mathcal{E}}_{k0}$ – absolute angular acceleration of T_k
 $\tilde{\mathcal{E}}_{k,k-1}$ – skew-symmetric matrix associated to the angular acceleration $\vec{\mathcal{E}}_{k,k-1}$
 $m_2^A = m_2^B = m$ – mass of each wheel
 $\hat{J}_2^A = \hat{J}_2^B = \hat{J}$ – symmetric matrix of tensor of inertia of each wheel
 $m_2^C = M$ – mass of central body

Department of Mechanics, “Politehnica” University of Bucharest

Rev. Roum. Sci. Techn. – Méc. Appl., Tome 56, N° 2, P. 113–126, Bucarest, 2011

\hat{J}_2^C – tensor of inertia of the central body about the link frame $C_2 x_2^C y_2^C z_2^C$
 M_1, M_2 – torques applied by two electric motors to the wheels jointed in A_2, B_2

1. INTRODUCTION

Wheeled mobile robots consist of a mobile platform and some cylindrical wheels, which roll with friction over a fixed or mobile surface. The condition of rolling without slipping and side slipping between the wheel and the contact surface demands the presence of non-holonomic constraints, which represent the kinematics model particularity of this kind of robot. The non-holonomic conditions reduce the number of degrees of mobility and hence most of robots have only two actuated joints: the two driven wheels.

These devices are needed nowadays in many applications: transport for material or tools over distances much larger than their dimensions, using in inaccessible places and in some agricultural workings, entertainment robots, service robots for domestic chores and for special medical proceedings, assertive devices for the mobility-challenged and rovers for interplanetary explorations. This is why the dynamics studies of these mobile systems gained more and more importance [1, 2, 3].

The Quasimoro prototype of the mobile wheeled-pendulum of Salerno and Angeles [4, 5] is a special quasi-holonomic mechanical system, which comprise two driving wheels and an intermediate body carrying the payload. Salerno, Ostrovskaya and Angeles studied in the paper [6] the dynamics of a rolling robot, using the second-order Lagrange equations with multipliers.

In order to cope with instability of the central body, the mass centre of the robot is particularly placed on the vertical axis passing through the midpoint of the line joining the wheel centres and *below* this line. The two main tasks of this robot are: positioning and orienting the payload, supported by the intermediate body on a flat surface (locomotion task) and stabilizing the oscillation of the intermediate body (stabilization task).

A literature survey on the two-wheeled robots led to two known systems: SCOUT [7] and Ginger-Segway [8]. For the inverted pendulum JOE (Grasser et al. [9]), a control system, made up of two-decoupled state-space controllers, pilots the motors so as to keep the system in equilibrium. In their paper, Nasrallah *et al.* [10] present the construction of a three-imbricated loop controller that delivers the full control strategy for the mobile-wheeled pendulum moving on an inclined plane. Pathak *et al.* [11] analyse the dynamics modelling and the position control of a series of wheeled inverted pendulum (Segway, Quasimoro, JOE) by partial feedback linearization and from a controllability point of view. Using a recursive formulation, the kinematics model with a global singularity analysis is carefully discussed in [12]. Chakraborty and Ghosal presented in their works [13, 14] the kinematics and a set of differential equations for the dynamics modelling and simulation of a wheeled mobile robot.

In the present paper we derive a dynamics model for the motion of two-wheeled mobile robots, using a matrix approach. We consider that the angular

displacements of the wheels and the rotation angle of the intermediate body determine the position and orientation of the robot. Using the principle of virtual powers or the Lagrange's equations of second kind, we formulate a matrix model of Quasimoro, which represents a two-input non-linear dynamical system with *three* outputs. This model is validated by means of simulations of dynamic responses of the system to different inputs and initial conditions. The results of the analysis are very important for the robot design and control. It turns out that the major disturbance in accomplishing tasks at hand is caused by the oscillations of the intermediate central body. Hence, the introduction of design corrections and the derivation of a suitable control algorithm should be considered in order to render the robot performances least sensitive to this disturbance [4, 10].

2. KINEMATICS MODEL OF THE ROBOT

Quasimoro is a wheeled mobile robot (*WMR*) consisting of two wheels of conventional type of same radius r , which are actuated by two independent motors, and of an intermediate central body that contains the control equipment, the actuation system, the power supply and the transmission mechanism. During motion both robot wheels can roll without slipping on a *horizontal* planarsurface and are assumed to be permanently in contact with this surface.

A *fictitious* horizontal platform, attached to the frame $C_2x_1y_1z_1$ of axis C_2x_1 linking the centres of the wheels, has a planar motion. Its position with respect to an inertial reference frame $Ox_0y_0z_0$ with the origin O fixed to the ground surface is given by the coordinates x_{10}, y_{10}, r and by the orientation angle ψ , which form the following matrices

$$\vec{r}_{10} = \begin{bmatrix} x_{10} \\ y_{10} \\ r \end{bmatrix}, \quad a_{10} = \begin{bmatrix} \cos \psi & \sin \psi & 0 \\ -\sin \psi & \cos \psi & 0 \\ 0 & 0 & 1 \end{bmatrix}. \quad (1)$$

Two cylindrical coaxial wheels linked to the frames $A_2x_2^Ay_2^Az_2^A$ and $B_2x_2^By_2^Bz_2^B$ are coupled to an intermediate body by means of revolute joints in points A_2 and B_2 (Fig. 1). They have known masses $m_2^A = m_2^B = m$ and the tensors of inertia

$$\hat{J}_2^A = \hat{J}_2^B = \hat{J} = \text{diag} \left[\frac{mr^2}{4}, \frac{mr^2}{4}, \frac{mr^2}{2} \right]. \quad (2)$$

A central cylinder of mass $m_2^C = M$ and tensor of inertia

$$\hat{J}_2^C = \text{diag} [J_1, J_2, J_3]. \quad (3)$$

is attached to the frame $C_2x_2^Cx_2^Cy_2^Cz_2^C$, which is jointed at the midpoint C_2 of line linking the mass centres of both wheels and represent the intermediate body.

$C_2x_1y_1z_1$, we obtain the following transformation matrices in the mobile reference frames [15, 16]:

$$a_{21}^A = a_z^{\theta_1} a_1, \quad a_{21}^B = a_z^{\theta_2} a_1, \quad a_{21}^C = a_z^{\theta_3} a_2, \quad (4)$$

where

$$a_1 = \begin{bmatrix} 0 & 0 & -1 \\ -1 & 0 & 0 \\ 0 & 1 & 0 \end{bmatrix}, \quad a_2 = \begin{bmatrix} 0 & 0 & -1 \\ 1 & 0 & 0 \\ 0 & -1 & 0 \end{bmatrix}, \quad a_z^{\theta_i} = \begin{bmatrix} \cos \theta_i & \sin \theta_i & 0 \\ -\sin \theta_i & \cos \theta_i & 0 \\ 0 & 0 & 1 \end{bmatrix}, \quad (i=1, 2, 3). \quad (5)$$

Defining $A_2B_2 = l$ the distance between the centres of the wheels and $C_2G = d$ the displacement of the centre G , following vectors give the invariable relative positions of the points A_2, B_2, C_2, G :

$$\vec{r}_{21}^{A_2} = [0 \quad \frac{l}{2} \quad 0]^T, \quad \vec{r}_{21}^{B_2} = [0 \quad -\frac{l}{2} \quad 0]^T, \quad \vec{r}_{21}^{C_2} = \vec{0}, \quad \vec{r}_2^{A_2} = \vec{0}, \quad \vec{r}_2^{B_2} = \vec{0}, \quad \vec{r}_2^G = [d \quad 0 \quad 0]. \quad (6)$$

The kinematics of the three elements is completely characterized by the translation velocity

$$\dot{\vec{r}}_{10} = [\dot{x}_{10} \quad \dot{y}_{10} \quad 0]^T \quad (7)$$

and by the angular velocities that are given below

$$\vec{\omega}_{10} = \dot{\psi} \vec{u}_3, \quad \vec{\omega}_{21}^A = \dot{\theta}_1 \vec{u}_3, \quad \vec{\omega}_{21}^B = \dot{\theta}_2 \vec{u}_3, \quad \vec{\omega}_{21}^C = \dot{\theta}_3 \vec{u}_3, \quad \vec{u}_3 = [0 \quad 0 \quad 1]^T \quad (8)$$

$$\omega_1 = \dot{\theta}_1, \quad \omega_2 = \dot{\theta}_2, \quad \omega_3 = \dot{\theta}_3, \quad \omega_\psi = \dot{\psi}.$$

The speed difference between the wheels generates rotation of the vehicles. Moreover, differentially driven robots can rotate on the spot.

Assuming that the two wheels roll without slipping on the ground surface, three analytical relations between the characteristic velocities of the three-degree-of-mobility robot express the non-holonomic constraints:

$$\vec{v}_{10} + \tilde{\omega}_{10} \vec{r}_{21}^{A_2} = [r \dot{\theta}_1 \quad 0 \quad 0]^T, \quad \vec{v}_{10} + \tilde{\omega}_{10} \vec{r}_{21}^{B_2} = [r \dot{\theta}_2 \quad 0 \quad 0]^T, \quad (9)$$

where

$$\vec{v}_{10} = a_{10} \dot{\vec{r}}_{10} = \begin{bmatrix} \dot{x}_{10} \cos \psi + \dot{y}_{10} \sin \psi \\ -\dot{x}_{10} \sin \psi + \dot{y}_{10} \cos \psi \\ 0 \end{bmatrix}, \quad \tilde{\omega}_{10} = a_{10} \dot{a}_{10}^T = \begin{bmatrix} 0 & -\dot{\psi} & 0 \\ \dot{\psi} & 0 & 0 \\ 0 & 0 & 0 \end{bmatrix}. \quad (10)$$

One of three analytical constrained relations (9) have been integrated:

$$\psi = \rho (\theta_2 - \theta_1), \quad \rho = \frac{r}{l}. \quad (11)$$

The above *conditions of connectivity* (9) can provide the matrix of the Jacobian and the characteristic velocities

$$\dot{\psi} = \rho (\dot{\theta}_2 - \dot{\theta}_1), \quad \dot{x}_{10} = \frac{r}{2} (\dot{\theta}_1 + \dot{\theta}_2) \cos \psi, \quad \dot{y}_{10} = \frac{r}{2} (\dot{\theta}_1 + \dot{\theta}_2) \sin \psi. \quad (12)$$

In order to determine the conditions of connectivity of accelerations we derive the matrix relations (9):

$$\ddot{\vec{r}}_{10} + (\tilde{\omega}_{10} \tilde{\omega}_{10} + \tilde{\varepsilon}_{10}) \vec{r}_{21}^{A_2} = [r \ddot{\theta}_1 \quad 0 \quad 0]^T + \tilde{\omega}_{10} [r \dot{\theta}_1 \quad 0 \quad 0]^T$$

$$\vec{\gamma}_{10} + (\tilde{\omega}_{10}\tilde{\omega}_{10} + \tilde{\varepsilon}_{10})\vec{r}_{21}^{B_2} = [r_1\ddot{\theta}_2 \ 0 \ 0]^T + \tilde{\omega}_{10}[r\dot{\theta}_2 \ 0 \ 0]^T, \quad (13)$$

where

$$\vec{\gamma}_{10} = a_{10}\ddot{\vec{r}}_{10} = \begin{bmatrix} \ddot{x}_{10} \cos \psi + \ddot{y}_{10} \sin \psi \\ -\ddot{x}_{10} \sin \psi + \ddot{y}_{10} \cos \psi \\ 0 \end{bmatrix}. \quad (14)$$

Thus, the characteristic accelerations $\ddot{\psi}$, \ddot{x}_{10} , \ddot{y}_{10} are immediately obtained:

$$\begin{aligned} \ddot{\psi} &= \rho(\ddot{\theta}_2 - \ddot{\theta}_1) \\ \ddot{x}_{10} &= \frac{r}{2}(\ddot{\theta}_1 + \ddot{\theta}_2) \cos \psi - \frac{r\rho}{2}(\dot{\theta}_2^2 - \dot{\theta}_1^2) \sin \psi \\ \ddot{y}_{10} &= \frac{r}{2}(\dot{\theta}_1 + \dot{\theta}_2) \sin \psi + \frac{r\rho}{2}(\dot{\theta}_2^2 - \dot{\theta}_1^2) \cos \psi. \end{aligned} \quad (15)$$

To describe the kinematical state of each body T_2^A , T_2^B , T_2^C with respect to fixed frame $Ox_0y_0z_0$, we express the angular velocity $\vec{\omega}_{20}$ and the linear velocity \vec{v}_{20} of the reference origin

$$\vec{v}_{20} = a_{21}(\vec{v}_{10} + \tilde{\omega}_{10}\vec{r}_{21}), \vec{\omega}_{20} = a_{21}\vec{\omega}_{10} + \vec{\omega}_{21}. \quad (16)$$

Performing the derivatives with respect to time of the equations (16), we obtain the accelerations $\vec{\gamma}_{20}$, $\vec{\varepsilon}_{20}$:

$$\vec{\gamma}_{20} = a_{21}\{\vec{\gamma}_{10} + (\tilde{\omega}_{10}\tilde{\omega}_{10} + \tilde{\varepsilon}_{10})\vec{r}_{21}\}, \vec{\varepsilon}_{20} = a_{21}\vec{\varepsilon}_{10} + \vec{\varepsilon}_{21} + a_{21}\tilde{\omega}_{10}a_{21}^T\vec{\omega}_{21} \quad (17)$$

and a useful characteristic square matrix [17]

$$\tilde{\omega}_{20}\tilde{\omega}_{20} + \tilde{\varepsilon}_{20} = a_{21}\{\tilde{\omega}_{10}\tilde{\omega}_{10} + \tilde{\varepsilon}_{10}\}a_{21}^T + \tilde{\omega}_{21}\tilde{\omega}_{21} + \tilde{\varepsilon}_{21} + 2a_{21}\tilde{\omega}_{10}a_{21}^T\tilde{\omega}_{21}. \quad (18)$$

3. EQUATIONS OF MOTION

3.1. PRINCIPLE OF VIRTUAL WORK

The torques $\vec{M}_1 = M_1\vec{u}_3$ and $\vec{M}_2 = M_2\vec{u}_3$, which are generated by two electric motors, transmit the motion at the two wheels. Having the direction of the common axis A_2B_2 , these moments can control the motion accomplished by the active wheels and the intermediate body. We will study the *direct dynamic problem*, in order to establish the evolution of the rotation angles θ_1 , θ_2 , θ_3 and the variation of the angular velocities $\dot{\theta}_1$, $\dot{\theta}_2$, $\dot{\theta}_3$ during the transient motion of $\Delta t = 1s$ between initial position and one, which correspond to other inactivated motion, knowing the torques M_1, M_2 . Thus, we will use the principle of virtual work.

Indeed, we assume that the two torque pulses of amplitudes M_1° and M_2° at an arbitrary instant are known by the following sinusoidal waveform functions

$$M_i(t) = M_i^\circ \sin \pi t \quad (i = 1, 2), \quad t \in [0, 1], \quad (19)$$

where, for example, $M_1^\circ = 0.1 \text{ Nm}$.

It is noteworthy that the simulation runs do not account for either external dissipation such as rolling friction between the wheels and ground and for internal dissipation such as friction in the bearings.

The fundamental principle of virtual work states that a mechanical system is under dynamic equilibrium if and only if the virtual work developed by all external, internal and inertia forces vanish during any general virtual displacement, which is compatible with the kinematical constraints [18, 19, 20].

The force of inertia and the resultant moment of the forces of inertia have the following general form

$$\vec{F}_{i0} = -m_i \{ \vec{\gamma}_{i0} + (\tilde{\omega}_{i0}^2 + \tilde{\varepsilon}_{i0}) \tilde{r}_i^G \}, \quad \vec{M}_{i0} = - \{ m_i \tilde{r}_i^G \tilde{\gamma}_{i0} + \hat{J}_i \tilde{\varepsilon}_{i0} + \tilde{\omega}_{i0} \hat{J}_i \tilde{\omega}_{i0} \} \quad (20)$$

where m_i is the mass and $\hat{J}_i = \oint \tilde{r}_i \tilde{r}_i^T dm_i$ represent the matrix definition of the tensor of inertia of body T_i .

The virtual velocities of the robot bodies result from relations (9) and (16), namely:

$$\begin{aligned} \omega_{1a}^v &= 1, \quad \omega_{2a}^v = 0, \quad \omega_{3a}^v = 0, \quad \omega_{10a}^v = -\rho \\ \vec{v}_{20}^{AT} &= [-r \sin \theta_1 \quad -r \cos \theta_1 \quad 0] \\ \vec{v}_{20}^{BT} &= [0 \quad 0 \quad 0] \\ \vec{v}_{20}^{CT} &= \left[\frac{r}{2} \sin \theta_3 \quad \frac{r}{2} \cos \theta_3 \quad 0 \right] \\ \vec{\omega}_{20}^{AT} &= [\rho \cos \theta_1 \quad -\rho \sin \theta_1 \quad 1] \\ \vec{\omega}_{20}^{BT} &= [\rho \cos \theta_2 \quad -\rho \sin \theta_2 \quad 0] \\ \vec{\omega}_{20}^{CT} &= [\rho \cos \theta_3 \quad -\rho \sin \theta_3 \quad 0]. \end{aligned} \quad (21)$$

The following matrix expression of the torque applied to the wheel A_2 results

$$M_1 = \vec{v}_{20}^{AT} \vec{F}_{20}^A + \vec{\omega}_{20}^{AT} \vec{M}_{20}^A + \vec{v}_{20}^{BT} \vec{F}_{20}^B + \vec{\omega}_{20}^{BT} \vec{M}_{20}^B + \vec{v}_{20}^{CT} \vec{F}_{20}^C + \vec{\omega}_{20}^{CT} \vec{M}_{20}^C, \quad (22)$$

with its definitive analytical form

$$\begin{aligned} M_1 &= A_{11} \ddot{\theta}_1 + A_{12} \ddot{\theta}_2 + A_{13} \ddot{\theta}_3 + A_{14} \dot{\theta}_1 \dot{\theta}_2 + A_{15} \dot{\theta}_2 \dot{\theta}_3 + A_{16} \dot{\theta}_3 \dot{\theta}_1 + \\ &\quad + A_{17} \dot{\theta}_1^2 + A_{18} \dot{\theta}_2^2 + A_{19} \dot{\theta}_3^2, \end{aligned} \quad (23)$$

where

$$A_{11} = 0.5mr^2(3 + \rho^2) + \rho^2(J_1 \cos^2 \theta_3 + J_2 \sin^2 \theta_3) + 0.25Mr^2$$

$$A_{12} = -0.5mr^2 \rho^2 - \rho^2(J_1 \cos^2 \theta_3 + J_2 \sin^2 \theta_3) + 0.25Mr^2$$

$$A_{13} = 0.5Mr d \cos \theta_3$$

$$A_{14} = Mr d \rho^2 \sin \theta_3$$

$$A_{15} = 2\rho^2 (J_1 - J_2) \sin \theta_3 \cos \theta_3 \quad (24)$$

$$A_{16} = -A_{15}, A_{17} = 0, A_{18} = -A_{14}$$

$$A_{19} = -0.5Mr d \sin \theta_3.$$

The relation (22) represent just the dynamics model of the *WMR*. The various dynamical effects, including the Coriolis and centrifugal forces coupling and the gravitational actions are considered in this explicit equation. Also, the results it has been verified in the framework of the Lagrange equations.

For the moment M_2 of the torque applied to the wheel B_2 we obtain an analogous final expression:

$$M_2 = A_{21}\ddot{\theta}_1 + A_{22}\ddot{\theta}_2 + A_{23}\ddot{\theta}_3 + A_{24}\dot{\theta}_1\dot{\theta}_2 + A_{25}\dot{\theta}_2\dot{\theta}_3 + A_{26}\dot{\theta}_3\dot{\theta}_1 + \\ + A_{27}\dot{\theta}_1^2 + A_{28}\dot{\theta}_2^2 + A_{29}\dot{\theta}_3^2, \quad (25)$$

where

$$A_{21} = A_{12}, A_{22} = A_{11}, A_{23} = A_{13} \\ A_{24} = A_{14}, A_{25} = A_{16}, A_{26} = A_{15} \\ A_{27} = A_{18}, A_{28} = A_{17}, A_{29} = A_{19}. \quad (26)$$

The third virtual displacement of the intermediate body correspond to the angular velocities

$$\omega_{3c}^v = 1, \omega_{1c}^v = 0, \omega_{2c}^v = 0, \omega_{10c}^v = 0. \quad (27)$$

After several transformations, following non-linear differential equation of third element T_2^C is obtained

$$A_{31}\ddot{\theta}_1 + A_{32}\ddot{\theta}_2 + A_{33}\ddot{\theta}_3 + A_{34}\dot{\theta}_1\dot{\theta}_2 + A_{35}\dot{\theta}_2\dot{\theta}_3 + A_{36}\dot{\theta}_3\dot{\theta}_1 + A_{37}\dot{\theta}_1^2 + \\ + A_{38}\dot{\theta}_2^2 + A_{39}\dot{\theta}_3^2 = M_1 + M_2 - Mgd \sin \theta_3, \quad (28)$$

where

$$A_{31} = 0.5Mr d \cos \theta_3, A_{32} = A_{31}, A_{33} = J_2 \\ A_{34} = -2(J_1 - J_2)\rho^2 \sin \theta_3 \cos \theta_3, A_{35} = 0 \\ A_{36} = 0, A_{37} = (J_1 - J_2)\rho^2 \sin \theta_3 \cos \theta_3 \\ A_{38} = A_{37}, A_{39} = 0. \quad (29)$$

3.2. EQUATIONS OF LAGRANGE

A solution of the dynamics problem of the mobile robots can be developed based on the Lagrange equations of second kind for a mechanical system with non-holonomic constraints. The generalized coordinates of the robot are represented by six parameters $q_1 = x_{10}$, $q_2 = y_{10}$, $q_3 = \psi$, $q_4 = \theta_1$, $q_5 = \theta_2$, $q_6 = \theta_3$.

The Lagrange equations with their multipliers $\lambda_1, \lambda_2, \lambda_3$ will be expressed by six differential relations

$$\begin{aligned} \frac{d}{dt} \left\{ \frac{\partial E}{\partial \dot{q}_k} \right\} - \frac{\partial E}{\partial q_k} &= Q_k + \sum_{s=1}^3 \lambda_s c_{sk} \quad (k=1, 2, \dots, 5) \\ \frac{d}{dt} \left\{ \frac{\partial E}{\partial \dot{\theta}_3} \right\} - \frac{\partial E}{\partial \theta_3} &= Q_6, \end{aligned} \quad (30)$$

which contain following six generalized forces

$$Q_1 = 0, \quad Q_2 = 0, \quad Q_3 = 0, \quad Q_4 = M_1, \quad Q_5 = M_2, \quad Q_6 = M_1 + M_2 - Mgd \sin \theta_3. \quad (31)$$

Three kinematical conditions of constraint given by the relations (9):

$$\sum_{k=1}^5 c_{sk} \dot{q}_k = 0 \quad (s=1, 2, 3) \quad (32)$$

can be concentrated in a matrix form, as follows

$$C \dot{\vec{q}} = 0, \quad (33)$$

where

$$\begin{aligned} C &= \begin{bmatrix} \cos \psi & \sin \psi & 0 & -r/2 & -r/2 \\ -\sin \psi & \cos \psi & 0 & 0 & 0 \\ 0 & 0 & l & r & -r \end{bmatrix} \\ \dot{\vec{q}} &= [\dot{x}_{10} \quad \dot{y}_{10} \quad \dot{\psi} \quad \dot{\theta}_1 \quad \dot{\theta}_2]^T. \end{aligned} \quad (34)$$

The components of the general expression of kinetic energy $E = \sum_{j=1}^3 E_j$ are

expressed as analytical functions of the generalized coordinates and their first derivatives with respect to time:

$$\begin{aligned} E_1 &= \frac{1}{8} mr^2 (6\dot{\theta}_1^2 + \dot{\psi}^2) \\ E_2 &= \frac{1}{8} mr^2 (6\dot{\theta}_2^2 + \dot{\psi}^2) \\ E_3 &= \frac{1}{2} m_3 (\dot{x}_{10}^2 + \dot{y}_{10}^2) + \frac{1}{2} (J_1 \cos^2 \theta_3 + J_2 \sin^2 \theta_3) + \\ &\quad + m_3 \dot{x}_{10} \dot{\theta}_3 d \cos \psi \cos \theta_3 + m_3 \dot{y}_{10} \dot{\theta}_3 d \sin \psi \cos \theta_3 - \\ &\quad - m_3 \dot{x}_{10} \dot{\psi} d \sin \psi \sin \theta_3 + m_3 \dot{y}_{10} \dot{\psi} d \cos \psi \sin \theta_3. \end{aligned} \quad (35)$$

A long and tedious calculus of the partial derivatives of all above functions leads to an algebraic system of six relations. In the direct or inverse dynamics problem, after elimination of the three multipliers, finally we obtain certainly same expressions (23), (25) for the torques M_1, M_2 required by the two driving wheels and same differential equation (28).

If the above complete equations (23), (25) do not take into account the rotation of the intermediate body of mass M , the expressions of two active torques M_1, M_2 for a symmetrical mobile robot can be written in the simplified form

$$\begin{aligned}
M_1 &= \frac{1}{4} Mr^2(\ddot{\theta}_1 + \ddot{\theta}_2) + \frac{1}{2} mr^2[3\ddot{\theta}_1 + \rho^2(\ddot{\theta}_1 - \ddot{\theta}_2)] + J_1 \rho^2(\ddot{\theta}_1 - \ddot{\theta}_2) \\
M_2 &= \frac{1}{4} Mr^2(\ddot{\theta}_1 + \ddot{\theta}_2) + \frac{1}{2} mr^2[3\ddot{\theta}_2 + \rho^2(\ddot{\theta}_2 - \ddot{\theta}_1)] + J_1 \rho^2(\ddot{\theta}_2 - \ddot{\theta}_1). \quad (36)
\end{aligned}$$

4. SIMULATIONS

Three important manoeuvres can be implemented:

1. *Rectilinear motion* with the angles $\psi = 0$, $\theta_1 = \theta_2$, accomplished by equal torques applied to the wheels

$$M_1 = M_2 = \frac{1}{2} (3m + M)r^2 \ddot{\theta}_1 + \frac{1}{2} Mrd(\ddot{\theta}_3 \cos \theta_3 - \dot{\theta}_3^2 \sin \theta_3) \quad (37)$$

and with one *differential equation*

$$J_2 \ddot{\theta}_3 + Mgd \sin \theta_3 + Mrd \dot{\theta}_1 \cos \theta_3 = 2M_1. \quad (38)$$

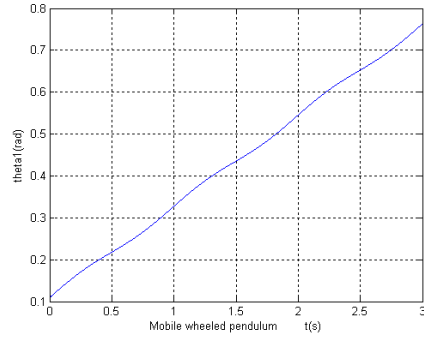
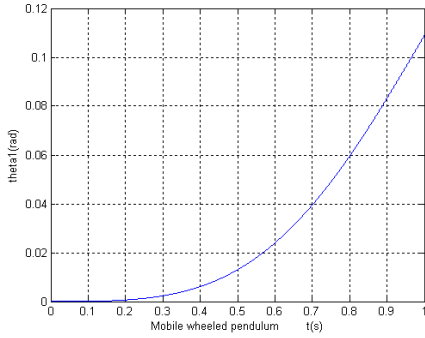


Fig. 2 – Actuated rectilinear motion: rotation angle θ_1 . Fig. 3 – Rectilinear motion: rotation angle θ_1 .

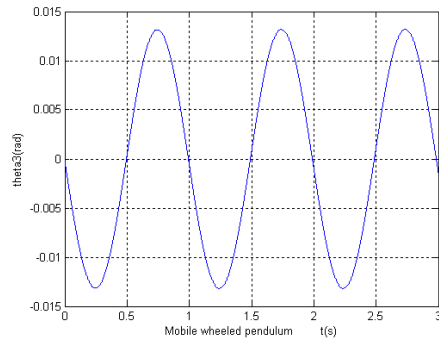
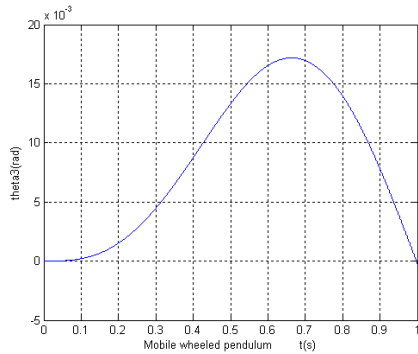


Fig. 4 – Actuated rectilinear motion: rotation angle θ_3 . Fig. 5 – Rectilinear motion: rotation angle θ_3 .

2. *Pure rotation* about the vertical axis passing through a fixed centre C_2 , with $\psi = -2\rho\theta_1$, $\theta_2 = -\theta_1$, $\theta_3 = 0$ and two equal torques, opposite in sign, applied to the wheels

$$M_1 = |M_2| = [mr^2(\frac{3}{2} + \rho^2) + 2\rho^2 J_1] \ddot{\theta}_1. \quad (39)$$

3. *Circular motion*, with a permanent angle $\theta_2 = 0$. During the first interval $\Delta t = 1$ s, the centre A_2 describes around the vertical axis $B_2 y_2^B$ a horizontal circle of radius $l = A_2 B_2$. As application, we will analyse the motion of a rolling robot, which has the following characteristics:

$$\begin{aligned} m &= 0.5 \text{ kg}, M = 5 \text{ kg}, J_1 = 0.2 \text{ kgm}^2, J_2 = 0.4 \text{ kgm}^2, \\ r &= 0.3 \text{ m}, d = 0.2 \text{ m}, \rho = 0.5. \end{aligned}$$

The response of the dynamical system subjected to two different inputs has been studied. These inputs will be represented by torques pulses (19), actuating the wheels for a duration of $\Delta t = 1$ s applied at $t_0 = 0$. Each simulation takes 90 s, but most of all outputs plots will be reported in the time window that goes from 0 s to $\Delta t + 3$ s, for example, to better show the transient response.

In every simulation the system is considered initially at rest. Three manoeuvres have been simulated:

1^o rectilinear motion, while maintaining constant the orientation angle $\psi = 0$; 2^o pure rotation about the vertical axis passing through C_2 , with $\theta_3 = 0$, *i.e.* vary the orientation angle ψ only; 3^o circular motion of centre A_2 around the axis $B_2 y_2^B$, with $\theta_2 = 0$.

1. *Rectilinear motion*. In this simulation run, two equal torque pulses (19) of amplitude $M_1^\circ = M_2^\circ = 0.1$ Nm are applied to the two wheels.

The outputs plots are reported in the following graphs: θ_1 (Fig. 2, Fig. 3) and θ_3 (Fig. 4, Fig. 5). The angles θ_1 , θ_2 and their first derivatives are equal, since the load condition is symmetric.

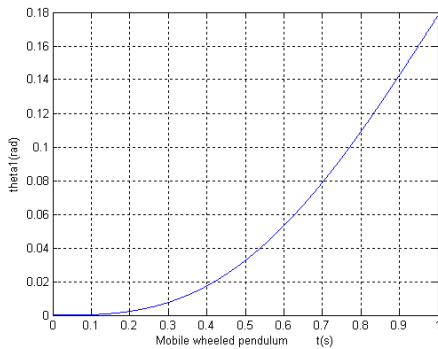


Fig. 6 – Actuated pure rotation: rotation angle θ_1 .

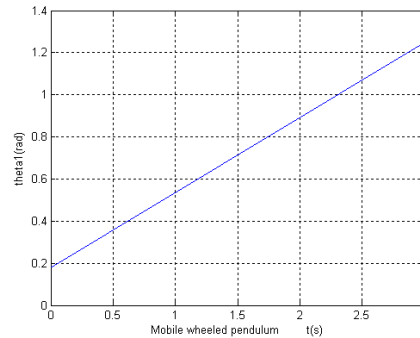


Fig. 7 – Pure rotation: rotation angle θ_1 .

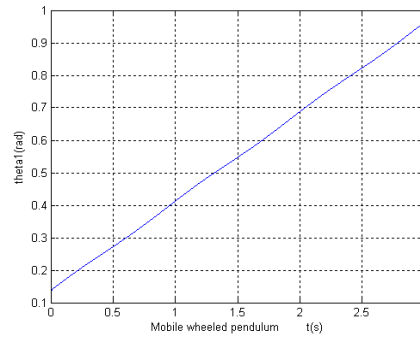
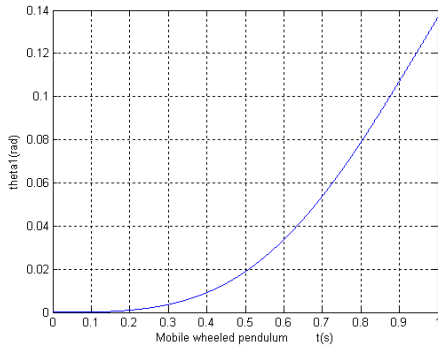


Fig. 8 – Actuated circular motion: rotation angle θ_1 . Fig. 9 – Circular motion: rotation angle θ_1 .

From Fig. 5, where θ_3 is represented by a periodic signal, we can infer that the oscillation of the intermediate body in the steady state is between -0.0129 rad and 0.0129 rad; of course, this theoretical oscillation needs no stabilization, since its amplitude is not big enough to be considered a disturbance for the accomplishment of the stabilization task. However, $\theta_3(0)$ might not be zero because of assembly and manufacturing errors; moreover, the actual surface on which the robot will move can be indeed slightly inclined [9].

The rectilinear trajectory is followed with high accuracy. Of course, the wheels will never experience the same torque in reality, which calls for a suitable control algorithm for accomplishment of the locomotion task. Moreover, a control algorithm is also needed because the velocity $\dot{x}_{10} = r\dot{\theta}_1$ along the rectilinear trajectory is not constant in the steady state.

2. *Pure rotation.* Two equal torque pulses $M_1 = -M_2 = M_1^\circ \sin \pi t$ of amplitude $m_1^\circ = 0.1$ Nm, opposite in sign, are applied to the wheels, during $\Delta t = 1$ s. The output plots are displayed in the following two graphs: θ_1 (Fig. 6, Fig. 7).

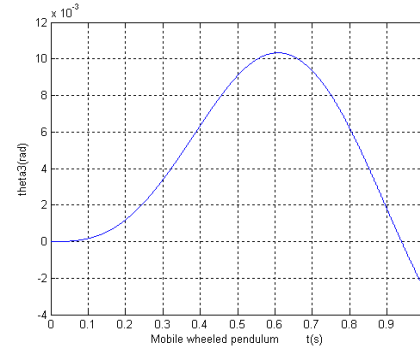
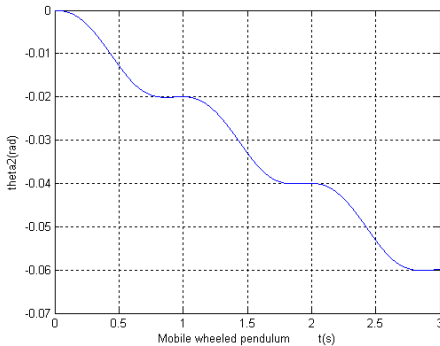


Fig. 10 – Circular motion: rotation angle θ_2 . Fig. 11 – Actuated circular motion: rotation angle θ_3 .

The trajectory of point C_2 reduces to a point coincident with the origin O of the inertial reference frame; moreover, the angular velocity $\dot{\theta}_1$ will be constant in

the steady state. Anyway, for what has been already stated about the errors affecting the construction of the robot, in reality the trajectory of point C_2 will not be a point; hence, a control algorithm for the accomplishment of the location task is needed [4]. For the assigned initial conditions and the type of input, the angle θ_3 and its first and second derivatives will remain theoretically equal to zero during the whole simulation, while θ_1, θ_2 and their derivatives are equal in amplitude and opposite sign.

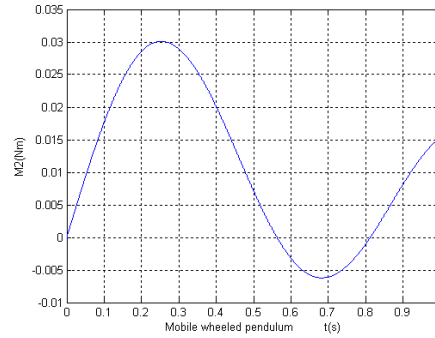
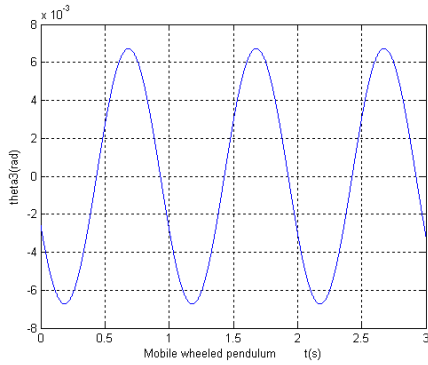


Fig. 12 – Circular motion: rotation angle θ_3 . Fig. 13 – Circular motion: torque of second wheel M_2 .

3. *Circular motion.* The torque $M_1(t) = 0.1 \sin \pi t$ applied to the first wheel is accompanied, in this third simulation, by a second unknown torque $M_2(t)$ applied to the other wheel. The outputs plots of this manoeuvre are reported in the graphs θ_1 (Fig. 8, Fig. 9), θ_2 (Fig. 10), θ_3 (Fig. 11, Fig. 12) and of course in the evolution of the torque M_2 (Fig. 13) applied to the second wheel.

5. CONCLUSIONS

1. Kinematics and dynamics of Quasimoro, a novel quasi-holonomic mobile robot, was discussed in the paper.

2. Based on the principle of virtual work, the present method establishes three differential non-linear equations for the rotation angles $\theta_1, \theta_2, \theta_3$. The dynamics model takes into consideration the mass, the tensor of inertia and the action of weight and inertia force introduced by each element of the mobile robot. The new approach is far more efficient, can eliminate all forces of internal joints and determine quickly the time-history evolution of torques and powers required by the driving wheels, in an eventual inverse dynamics problem.

3. We formulated the mathematical model of the mechanical system and provided a numerical validation of it. The simulation through the software MATLAB program certify that one of the major advantages of the current matrix recursive formulation is a reduced number of additions or multiplications and consequently a smaller processing time of numerical computation in comparison with the approach based on the Lagrange equations.

REFERENCES

1. S.K. SAHA, W.O. SCHIEHLEN, *Recursive kinematics and dynamics for parallel structured closed-loop multi-body systems*, Mech. Struct. and Mach. **29**, 2, pp. 143-175, 2001.
2. R. COLBAUGH, M. TRABATTI, K. GLASS, *Redundant nonholonomic mechanical system: characterization and control*, Robotica, Cambridge University Press, **17**, 2, pp. 203-217, 1999.
3. P.F. MUIR, C.P. NEUMAN, *Kinematic modeling of mobile robots*, Journal of Robotic Systems **4**, 2, pp. 281-304, 1987.
4. A. SALERNO, J. ANGELES, *On the nonlinear controllability of a quasiholonomic mobile robot*, Proceedings of the IEEE International Conference on Robotics and Automation ICRA'2003, pp. 3379-3384, Taipei, Taiwan, 2003.
5. A. SALERNO, J. ANGELES, *A new family of two-wheeled mobile robots: modelling and controllability*, IEEE Transactions on Robotics, **23**, 1, pp. 169-173, 2007.
6. A. SALERNO, S. OSTROVSKAYA, J. ANGELES, *The Dynamics of a Novel Rolling Robot-Analysis and Simulation*, Proceedings of the 11th World Congress in Mechanism and Machine Science, Tianjin, China, 2004, pp. 1956-1960.
7. A. DRENNER, I. BURT, T. DAHLIN, B. KRATOCHVIL, C. Mc MILLEN, B. NELSON, N. PAPANIKOÏPOULOS, P.E. RYBSKI, K. STUBBS, D. WALETZKO, K. BERK YESIN, *Mobility enhancements to the SCOUT robot platform*, Proceedings of the IEEE International Conference on Robotics & Automation, Washington D.C., USA, 2002.
8. D.I. KAMEN, R.R. AMBROGI, R.J. DUGGAN, D.J. FIELD, R.K. HEINZMANN, B. AMSBURY, C.C. LANGENFELD, *Personal mobility vehicles and methods*, Patent, PCT/US00/15144, 2000.
9. F. GRASSER, A. D'ARRIGO, S. COLOMBI, A.C. RUFER, *JOE: A Mobile Inverted Pendulum*. IEEE Transaction on Industrial Electronics, **49**, 1, pp. 107-114, 2002.
10. D.S. NASRALLAH, J. ANGELES, H. MICHALSKA, *Position and Orientation Control of a Mobile Wheeled Pendulum Moving on an Inclined Plane*, Proceedings of the IEEE International Conference on Mechatronics ICM'2006, 2006, pp. 426-431, Budapest, Hungary.
11. K. PATHAK, J. FRANCH, S.K. AGRAWAL, *Velocity and position control of a wheeled inverted pendulum by partial feedback linearization*, IEEE Transactions on Robotics, **21**, 3, pp. 505-513, 2005.
12. L. GRACIA, J. TORNERO, *Kinematic modelling and singularity of wheeled mobile robots*, Adv. Robotics, Cambridge University Press, **21**, 7, pp. 793-816, 2007.
13. N. CHAKRABORTY, A. GHOSAL, *Kinematics of wheeled mobile robots on uneven terrain*, Mechanism and Machine Theory, Elsevier, **39**, 12, pp. 1273-1287, 2004.
14. N. CHAKRABORTY, A. GHOSAL, *Dynamic Modelling and Simulation of a Wheeled Mobile Robot for Traversing Uneven Terrain Without Slip*, Journal of Mechanical Design, **127**, 5, pp. 901-909, 2005.
15. S. STAICU, *Dynamics equations of a mobile robot provided with caster wheel*, Nonlinear Dynamics, Springer, **58**, 1-2, pp. 237-248, 2009.
16. S. STAICU, X-J. LIU, J. WANG, *Inverse dynamics of the HALF parallel manipulator with revolute actuators*, Nonlinear Dynamics, Springer, **50**, 1-2, pp. 1-12, 2007.
17. S. STAICU, D. ZHANG, *A novel dynamic modelling approach for parallel mechanisms analysis*, Robotics and Computer-Integrated Manufacturing, Elsevier, **24**, 1, pp. 167-172, 2008.
18. S. STAICU, X-J. LIU, J. LI, *Explicit dynamics equations of the constrained robotic systems*, Nonlinear Dynamics, Springer, **58**, 1-2, pp. 217-235, 2009.
19. S. STAICU, *Dynamics analysis of the Minuteman cover drive*, European Journal of Mechanics – A/Solids, Elsevier, **29**, 1, pp. 91-96, 2010.
20. S. STAICU, *Dynamics of the 6-6 Stewart parallel manipulator*, Robotics and Computer – Integrated Manufacturing, Elsevier, **27**, 1, pp. 212-220, 2011.